Fall 2019

A Foundation for Understanding the Neurocognitive Processes That Underlie Mathematics Performance in Children

Christopher Anzalone

A FOUNDATION FOR UNDERSTANDING THE NEUROCOGNITIVE PROCESSES THAT UNDERLIE MATHEMATICS PERFORMANCE IN CHILDREN

By

Christopher Anzalone

Bachelor of Science
University of Rochester, 2015

Submitted in Partial Fulfillment of the Requirements

For the Degree of Master of Arts in

School Psychology

College of Arts and Sciences

University of South Carolina

2019

Accepted by:

Scott Decker, Director of Thesis

Jessica Green, Reader

Cheryl L. Addy, Vice Provost and Dean of the Graduate School

ABSTRACT

The current study investigated the prognostic utility of resting state EEG coherence in the prediction of standardized mathematics scores. Quantitative EEG analyses were performed for 60 school-aged children (ages 7 to 12 years) with and without math learning disabilities (MLD). Analyses assessing intrahemispheric coherence at rest were performed across the entire sample and several coherence networks were extracted. Specifically, networks that included Brodmann area 40 (BA 40) -- a region of the brain heavily involved in the cognitive processes responsible for mathematics performance (Anderson, Betts, Ferris, & Fincham, 2011; Cohen, Dehaene, Chochon, Lehericy, & Naccache, 2000; Kroger, Nystrom, Cohen, & Johnson-Laird, 2008) -- and whose coherence was significantly correlated with standardized math scores were examined. Results indicated that there was a total of four coherence networks, two in each hemisphere, that had prognostic utility for math ability. These networks included coherence in multiple frequency bands between BA 40 and several other brain regions (left frontotemporal cortex in delta, left occipitotemporal cortex in theta, whole right hemisphere in alpha, and right medial prefrontal cortex in theta). These findings address a relatively large void in the research literature as there are few studies investigating the neurological foundations of mathematics in children. Further, these results lend credence for the supplementary use of EEG for identifying specific learning disabilities in addition to providing a basis for which interventions can be targeted toward.

TABLE OF CONTENTS

LIST OF TABLES

LIST OF FIGURES

CHAPTER 1

INTRODUCTION

Mathematical reasoning is perhaps one of the most vital cognitive skills a child must master (Rivera, Reiss, Eckert, & Menon, 2005). Children who fail to learn math have a life-long handicap that can substantially impact daily living well into adulthood (Garnett, 1998; Ritchie & Bates, 2013). The societal myth that it is acceptable for a person to be inept at math is challenged, as is exhibited by individuals who experience math deficits well into adulthood (Johnson & Blalock, 1987). Adults who have not obtained proficient mastery of basic math skills often struggle in various occupational prospects as well as in many other activities of daily living. For these reasons it is crucial for clinicians to have the ability to adequately and efficiently identify individuals who may be in need of math interventions early on in their lives. Although recently, school systems have made strides to improve their ability to identify students with specific learning disabilities (SLDs), there is still much room for growth and improvement.

It is estimated that 3-8% of students suffer from a form of math disability worldwide, though estimates vary depending on how researchers operationalize and define the disorder (Van Luit & Toll, 2018). The current approaches used to identify children with math learning disabilities (LDs), as guided by U.S. federal and state legislation, have significant problems (Decker et. al 2012; Fletcher, et. al, 2007). Identification approaches that are currently relied upon, such as the IQ-Discrepancy Model, referred to as a “wait-to-fail” approach, can only be deployed for children after

they have fallen far behind in a subject; this normally results in years of intervention to merely catch up to peers. The alternative approach, Response to Intervention, which was designed to address this problem and improve early identification, does not lead to improved outcomes (Balu et al., 2015). Although an RTI method theoretically enhances early intervention, failure to respond to an intervention does not provide sufficient diagnostic information to identify a disability. As such, the potential for supplementary and more reliable methods to identify children with math LDs exists and should therefore be pursued.

A likely reason for the issues seen regarding improper diagnosis and intervention for children with specific learning disabilities can be explained by the relatively large gap in the neurocognitive research literature on these topics. Clinicians and researchers alike have continued to make strides toward improving our understanding of the neurological underpinnings of specific learning disorders, but no research to date has explored neuroimaging as a way to help characterize a child's potential for specific sets of mathematical skills.

By having models of brain activity that predict a child's aptitude for math skills, clinicians can provide interventions aimed to specifically target the underlying cognitive mechanisms responsible for observed deficits. For example, it may be determined that a student with poor Calculation scores on the WJ-III has a deficit in math calculation skills, but in actuality, this student may have abnormal brain coherence between the brain structures responsible for cognitions such as number sense and executive functioning, attention, or even vision. By having data obtained directly from a child's brain, examiners can more broadly assess a child's cognitive functioning as it pertains to specific math

skills. This can assist in the formulation of additional, potentially more accurate, hypotheses to explain poor math performance, and thus lead to a more effective identification and intervention process.

Guided by fMRI research examining the neurocognitive mechanisms involved in math performance (Arsalidou & Taylor, 2011; Dehaene & Cohen, 1995; Dehaene, 1992) and qEEG research examining coherence and mathematical performance (González-Garrido et al., 2018), the current study aims to add to the literature by examining the predictive utility of qEEG coherence on general and specific math skills. Because BA 40 has been established as an essential brain area for mathematics performance (Arsalidou & Taylor, 2011), the current study examines how brain connectivity with this region at rest can predict a child's aptitude for math skills. This information can augment our understanding of the underlying neurocognitive mechanisms fundamental to mathematical ability and thus, guide future research on academic assessment batteries as well as math interventions for struggling children.

The current study utilizes EEG imaging techniques because they offer a number of advantages over other imaging modalities for studying the neurocognitive factors implicated in academic performance. First, EEG research methods are relatively easy to use and they incur few financial expenses relative fMRI, second, EEG's temporal resolution is significantly greater than that other brain imaging modalities (Burle et al., 2015), and finally, EEG has the potential for therapeutic applications through the use of neurofeedback therapy. Consequently, there is a growing interest for the use EEG in both the research and clinical domains of healthcare, though the extant research literature on MLDs largely comprises of fMRI imaging techniques. As such, using EEG to study

mathematical skills offers up the potential for growth in many spheres of psychological clinical practice and research. By utilizing EEG, the current study fills a gap in the research literature centered on the neurocognitive processes involved in math while surpassing the practical and methodological limitations of studies that utilize fMRI.

Despite the growing literature base and large potential for EEG applications to provide a better understanding of math abilities, more research is needed. Early studies on the utility of EEG recognized that, in addition to the more routine analyses, coherence analyses might further yield valuable information about brain functioning (Dumermuth, 1973). Coherence, in the context of EEG, refers to the degree of brain activity synchrony between specified locations throughout the brain (Gasser, Jennen-Steinmetz, & Verleger, 1987). Thus, coherence, in principle, can be used to determine which brain networks are active during the EEG recording and which general brain regions are involved in those particular networks. A coherence recording at rest (subject not performing a task) would imply a recording of the individual's basal electrophysiological brain functions, which has been termed the "EEG-Default Mode Network" (Chen, Feng, Zhao, Yin, & Wang, 2008). Examining an individual's default brain activity can provide information about their neurocognitive aptitudes or, in some cases, incapacities (Margolis, Pagliaccio, Thomas, Banker, & Marsh, 2019; Rocca et al., 2010; Savini et al., 2019), thus the current study proposes a method for examining children's resting state brain networks and utilizing the degree of coherence among them to characterize their potential for mathematics performance.

Neuroimaging and Math

Staggering progress has been made in the past several decades with regards to neurocognitive and brain science research. Methodological, statistical, software, and hardware advances over the last several years has facilitated this progress, which has fostered immense interest among researchers and medical practitioners (Plerou & Vlamos, 2016). With the mounting interest in neuroscience research, our ability to test theories and gain insight into the underpinnings of human cognition has continued to augment.

FMRI.

In 1992, Dehaene (1992) proposed a theoretical model of mental arithmetic and numerical processing entitled "the triple-code model". Three years later – with the advent of fMRI and its corresponding research studies thoroughly underway – Dehaene & Cohen (1995) expanded upon this model by reviewing the extant fMRI case studies on this topic. Dehaene and Cohen sought to better understand the neuroanatomical brain regions involved in processing mathematical problems. Through their review of the relevant fMRI research, they expanded upon the triple-code model to create a cohesive functional-anatomical model of number and arithmetic mental processing. This updated model hypothesized the anatomical correlates of mathematical ability and number processing. Specifically, their updated triple-code model theorizes that numbers are processed by three distinct brain areas: (1) visual number processing occurs in the ventral occipitotemporal areas, (2) quantity and magnitude judgements occur in the inferior parietal areas (Brodmann's area 40), and (3) the left perisylvian areas in the inferior parietal lobules process the mathematical verbal code. The model has since been

empirically validated (Schmithorst & Brown, 2004) and further expanded upon with the availability of additional fMRI data (Arsalidou & Taylor, 2011).

In order to update Dehaene's 1995 model, Arsalidou & Taylor (2011) conducted a quantitative meta-analysis of 34 fMRI studies in healthy children below the age of 14. Their study further validates Dehaene's model, and proposes an atlas of functional anatomical correlates for mental arithmetic operations. Statistical analyses calculating the activation likelihoods during math tasks across all 34 studies indicate that both the left and right inferior parietal lobules (Brodmann's area 40: BA 40) were the most likely brain regions to show activation during general numerical processing and calculation tasks. BA 40 showed a relatively high likelihood of activation during addition tasks, a moderate activation likelihood during subtraction tasks, and a relatively low likelihood for activation during multiplication tasks (Arsalidou & Taylor, 2011). These findings suggest that the cognitive processes specialized to BA 40 play a crucial role in children's ability process numbers and perform simple mental calculations, a finding that further supports the theories first presented in Dehaene's functional-anatomical triple-code model.

QEEG.

Quantitative electroencephalography (qEEG) has an extensive history of being used to assess underlying brain functions for various neuropsychological disorders. For example, results from several studies have demonstrated that qEEG measures can accurately discriminate between individuals who have experienced a TBI and those who have not. Thatcher, Walker, Gerson, & Geisler (1989) report that qEEG was able to differentiate TBI patients from non-TBI patients with 90%-95% accuracy. Further studies

utilizing qEEG provide evidence to support its utility for classifying TBI severity with 96% accuracy (Thatcher et al., 2001a). Numerous other studies have also utilized qEEG measures to examine their relationship with measures of intelligence, several of them reporting significant relationships between coherence and standardized intelligence measures (Neubauer & Fink, 2009; Thatcher, North, & Biver, 2005; Martín-Loeches, Muñoz-Ruata, Martínez-Lebrusant, & Gómez-Jarabo, 2001;). Additional studies have further supported utilizing qEEG for studying neuropsychological differences in individuals with ADHD, demonstrating its utility in this domain with several decades worth of literature (Barry, Clarke, Johnstone, McCarthy, & Selikowitz, 2009; Clarke, Barry, McCarthy, & Selikowitz, 1998, 2001; Janzen, Graap, Stephanson, Marshall, & Fitzsimmons, 1995; Satterfield, Cantwell, Lesser, & Podosin, 1972).

Despite an extensive history of utilizing qEEG for studying various neurocognitive phenomena, a relatively small base of literature exists outlining its utility for examining children's academic skills and abilities. While recent EEG studies have begun to focus on children's reading abilities and disorders (e.g. dyslexia) (Arns, Peters, Breteler, & Verhoeven, 2007; Lehongre, Morillon, Giraud, & Ramus, 2013; Rippon & Brunswick, 2000), very few studies examining the cognitive mechanisms involved in specific mathematics skills exist.

While arithmetic abilities have been studied for many years within the frame of an educational context, neurocognitive research on mathematics abilities is a relatively recent field of study (Plerou & Vlamos, 2016). Contemporary research literature exploring the utility of qEEG as it relates to mathematics skill and ability is scarce, though mounting. One of the most recent research studies on this topic, done by

González-Garrido et al. (2018), explores mathematical achievement as it relates to qEEG measures of coherence. Specifically, this study aimed to evaluate coherence levels in children with differing math skill levels while they performed a math related task. Interestingly, results of this study indicate that there are electrophysiological brain differences between children who are adept at math and those who are not.

González-Garrido et al. (2018) examined coherence to assess brain function. Coherence is type of qEEG analyses often used when investigating EEG data (John, Prichep, Fridman, & Easton, 1988; Thatcher, North, & Biver, 2005a; Thatcher et al., 2001b, 1989). It provides a measure of the phase angle consistency between two brain regions in a set of continuous EEG data (Thatcher, North, & Biver, 2005b). Essentially, coherence is a quantitative value representing a denotation of regions in the brain that are oscillating at the same frequency simultaneous to one another. Thus, examining the coherence among brain regions can provide valuable information with regards to functional brain connectivity and cognitive functioning (González-Garrido et al., 2018).

Utilizing coherence to examine mathematical achievement, González-Garrido et al.'s 2018 study suggests that, although there are no coherence networks specific to mathematics, children's mathematical abilities likely rely upon a complex integration of several interconnected brain networks. This theory is in support of findings from prior research depicting EEG differences during different mental calculation tasks (Fernández et al., 1995). Models from González-Garrido et al.'s 2018 study expand further to propose that high achieving (HA) children display more localized coherence over parietal areas than low achieving (LA) children, thus, children with a greater amount of connectivity near BA 40 will likely fair better in mathematics than those who have less. The authors of

the study hypothesized that this observation might reflect a more developed numerical processing skills system, arising from more specialized brain networks for numeric processing.

Cognitive Deficits in Math Disabilities

Dyscalculia is characterized by having a difficulty in learning or comprehending arithmetic. This includes deficits in understanding and conceptualizing numbers and magnitudes, learning how to manipulate numbers, and learning mathematical facts (Plerou & Vlamos, 2016). Research findings suggest that math disabilities can be highly indiscriminant, affecting students with average intelligence, while also affecting those with global developmental and/or learning disorders (Van Luit & Toll, 2018). Several associative cognitive factors have been described in order to operationalize math learning problems. Interestingly, these factors can all be linked to the functional properties of BA 40. These cognitive factors include deficits in planning skills and attention (aspects of executive functioning), naming speed, working memory, and number sense (Van Luit & Toll, 2018).

Planning processes are required during math tasks for choosing and applying correct computational strategies, monitoring calculations, applying prior mathematical knowledge, and appropriately checking answers (Hiebert & Lefevre, 1986). Similarly, the ability to maintain *attention and focus* throughout a math related task ensures that the individual is accurately representing the math problem throughout the computational processes (Passolunghi & Cornoldi, 2000). Thus, an adequate level of executive function abilities is a vital component for completing mathematical tasks as well as properly learning math related procedures and concepts.

Naming speed is an indirect method of assessing individuals' ability to access and retrieve information from long-term memory (Van Luit & Toll, 2018). Students who exhibit weaknesses in naming speed tasks could indicate that they experience difficulty in retrieving mathematical information from memory. If there are deficits in naming speed for numbers, this can indicate that more cognitive resources and effort are required to complete math related tasks. Likewise, general naming speed deficits can indicate more global cognitive deficits, ones that may give rise to deficits related to mathematical performance (Koponen, Georgiou, Salmi, Leskinen, & Aro, 2017).

As is true with most – if not all – academic skills, *working memory* is a crucial cognitive component for performing math related tasks (Toll, Van der Ven, Kroesbergen, & Van Luit, 2011). Especially during math tasks, large amounts of information must be retained and processed. In order to process the information effectively and efficiently heavy demands are placed upon one's working memory. As such, a student who experiences difficulties in storing, updating, and reproducing verbal procedures as well as visual spatial information can exhibit deficits in math performance (Berg, 2008; D'Amico & Guarnera, 2005).

Number sense -- a construct that has been described as a foundational ability for learning mathematics -- refers to the ability to process and accurately conceptualize numeric qualities and magnitudes (Gersten & Chard, 1999). Several studies have shown that a child's number sense can be a predictive factor for overall mathematical skills (Mazzocco, Feigenson, & Halberda, 2011; Mussolin, Mejias, & Noël, 2010; Piazza et al., 2010). Deficits in this domain point to an underlying cognitive weakness that can lead to serious math performance problems (Butterworth, Varma, & Laurillard, 2011).

Brodmann's Area 40

The function of Brodmann's area 40, synonymously referred to as the inferior parietal lobule (IPL), has been extensively studied, though many of its theorized functions remain contested (Andersen, 1987; Mattingley, Husain, Rorden, Kennard, & Driver, 1998). Researchers have argued that this brain region plays crucial roles in spatial perception, visual motor integration (Andersen, 1987), tactile perception, manual construction (Jäncke, Kleinschmidt, Mirzazade, Shah, & Freund, 2001), working memory (Baldo & Dronkers, 2006), decision making (Vickery & Jiang, 2008), sustained attention (Singh-Curry & Husain, 2009), and – most notably for the purposes of this study – mental mathematical operations (Anderson, Betts, Ferris, & Fincham, 2011; Cohen, Dehaene, Chochon, Lehericy, & Naccache, 2000; Kroger, Nystrom, Cohen, & Johnson-Laird, 2008).

Several techniques have been used to study the functionality of this brain region. Lesion studies indicate that patients who have suffered damage to the IPL often suffer from multiple syndromes including aphasia, dyslexia, visual-spatial neglect, and dyscalculia (Cohen et al., 2000; Singh-Curry & Husain, 2009). Neuroimaging research on the IPL further supports the results from lesion studies, providing evidence that the IPL plays a critical role in language and calculation abilities (Cohen et al., 2000; Rivera et al., 2005). Interestingly, Rivera et al.'s (2005) study suggests that children who are more adept in math have greater activation in BA 40 with less activation in other regions compared to children less proficient in math. The authors of that study theorized that this is evidence to suggest a functional specialization for mental arithmetic processes for BA 40.

Current Study

Although progress has been made in understanding the underlying cognitive processes and their corresponding brain structures that may be implicated in mathematical abilities (Arsalidou & Taylor, 2011), clinicians in the field still struggle to use this information in applied contexts (Plerou & Vlamos, 2016). Since the field has made great strides over the past decade in understanding the neurological underpinnings of mathematical skills, more research is needed to help us to apply this knowledge in clinical contexts (Plerou & Vlamos, 2016).

The current study aims to utilize qEEG to explore children's default brain activity. The goal is to determine if the existence of certain brain networks, and the strength of coherence within them, can predict general and specific math skills. By gathering continuous sets of EEG data from participants and extracting coherence values the current study examines intrahemispheric connectivity, specifically between BA 40 and other BAs. Determining brain regions that are significantly coherent with BA 40 allows us to identify brain networks that can be linked to specific math abilities (Anderson et al., 2011; Cohen et al., 2000; Kroger et al., 2008). We may then assess each of these networks to determine if the levels of coherence (connectivity) among them provide value in predicting sets of math skills (as measured by standardized math composite scores of Calculation, Applied Problems, and Math Fluency from the WJ-III Ach).

Confirming the existence of bio-signatures for specific sets of math skills, such as the ones outlined above, allows researchers and clinicians to be better equipped to assess and clarify true math disabilities from secondary cognitive disorders that affect math

performance. This will lead to the development of more appropriate interventions for children who experience deficits in mathematics performance, ones targeted directly toward the etiology of the deficiencies. To obtain these bio-signatures, practitioners would simply administer a non-invasive EEG over the course of a few minutes. The qEEG data would be integrated with standard psychoeducational assessment data to formulate a complete cognitive profile of each child. The identification neurocognitive factors implicated in math performance (e.g. network coherence) enables a more comprehensive, integrated depiction of an individual student's learning and performance profile – and thus, a more thorough basis for appropriate interventions should math performance weaknesses be observed.

CHAPTER 2

METHOD

Participants

Participants for the current study included 60 school-aged children (ages 7 to 12 years), with the goal of collecting data on a sample of children who represent the full range of math standard scores. In order to ensure the full range of mathematical achievement scores was obtained in the sample, those with a suspected and/or confirmed MLD were recruited as well as those without. Children were recruited through local advertisements and agencies in the Columbia, SC area that serve children with MLD. Specifically, the Sandhills School for Learning Disabilities and Tutor Eau Claire were the primary agencies where recruitment efforts were directed.

The inclusion criteria for the MLD portion of the study sample consisted of: 1) appropriate age (7-12 years), 2) currently and/or previously identified as a child with a specific learning disability in math (i.e. provide documentation from their school), and/or 3) score below the 25th percentile on the WJ-III Ach Math Calculation test and/or Math Fluency test. At the end of recruitment, 30 children were included in the MLD sample. Inclusion criteria for the other portion of the study sample (i.e., typically developing children, without math learning difficulties) consisted of: 1) no current or previous IEP in school or qualification for special education services, and 2) score at or above the 25th percentile on the WJ-III Ach Math Calculation and Math Fluency tests. This sample consisted of an additional 30 children. Children were excluded from the study if they

were deemed to have an intellectual disability, as determined by their Broad Cognitive Ability score from the WJ-III Cog falling below the score of 70. Descriptive statistics for the overall sample, collapsed across both groups are included in Table 2.1.

Measures

The current study used the Woodcock-Johnson Tests of Achievement in order to determine mathematical abilities. This battery is designed to measure an individual's academic skills who are aged two to 90 or more years, and it has been validated for its reliability and consistency in research studies. Its core subtests have median reliability coefficients of r_{11} = .81 - .94 (Note, the Broad Cognitive Ability score on the WJ-III Cog was used as an estimate of IQ, to rule-out general cognitive impairment for children scoring low on math measures used in the inclusion criteria)

EEG data was collected to examine whether specific frequency bands (i.e. delta, theta, alpha 1, alpha 2, beta 1, beta 2, beta 3, and high-beta) and the coherence patterns within them were able to predict the degree of a child's mathematical ability. EEG data was recorded from 19 channel electrodes distributed across the scalp via Electro-cap (references to nasion and inion) using the 10/20 placement system. The standard placement of each of the 19 electrodes is illustrated in Figure 2.1. FP1 and FP2 are electrodes placed over the prefrontal cortex, while F3, F4, F7, and F8 are electrodes placed over the frontal lobe. Electrodes T3, T4, T5, and T6 are placed over the temporal lobe, while the parietal lobe has electrodes P3 and P4. O1 and O2 are placed over the occipital lobe. FZ, CZ, and PZ measure midline brain activity, while C3 and C4 are placed between the temporal lobe to measure centro-temporal brain activity. Finally, A1 and A2 within Figure 2.1 represent ground leads (i.e., ear clips).

Data was sampled at 1026 Hz using a BrainMaster Discovery 24E amplifier. This device was selected due to its FDA approval classification as well as its compatibility with the Neuroguide program 6.6.4 (Thatcher, 2011). A 60Hz notch filter was used to removed noise caused by electronics from the surrounding environment and the bandwidth range was set to record frequencies between 1.0 and 30 Hz. The frequency bands used in the current study are defined as follows: delta (1.0 - 4.0 Hz), theta (4.0 - 8.0 Hz), alpha 1 (8.0 -10.0 Hz), alpha 2 (10.0 - 12.0 Hz), beta 1 (12.0 - 15.0 Hz), beta 2 (15.0 - 18.0 Hz), beta 3 (18.0 - 25.0 Hz), and high-beta (25.0 - 30.0 Hz). Impedance values for the A1 and A2 ear reference electrodes were kept below 5KΩ, and all other electrode impedance values were kept below 10KΩ for all subjects. Neuroguide 6.6.4 (Thatcher, 2011) was used for removing EEG artifact in the data and to obtain normative values of qEEG spectral coherence. MATLAB 2018a (*MATLAB*, 2018) was used for data transformation and organization.

Procedures

Data used in the current study was derived from a prior research study aimed at examining the relationships between brain function, math performance, and anxiety. Prior to conducting the study, approval to perform the research procedures was granted from the University of South Carolina's institutional review board. Participants were provided child assent and parental consent forms and signatures were obtained. Preliminary measures of mathematical skills and cognitive abilities were obtained from participants who agreed to partake in the study. Specifically, the WJ-III Ach and WJ-III Cog measures were administered. Data from participants who met the study eligibility criteria were retained and EEG data were recorded.

EEG recordings were obtained by fitting the participants with their appropriately sized Electro-Cap and ground leads (as described previously). The recordings were collected over three-minute intervals while the participants' eyes were closed. All data used for the current study were collected over the course of one to two study sessions. Following data collection procedures, participant data was de-identified (i.e. participants' names were replaced with study ID numbers) to protect their confidentiality.

Data Analysis

Several procedures were required to allow for qEEG analyses to be performed. Prior to conducting analyses, the first minute of each participant's qEEG data was manually inspected to identify a minimum of ten seconds of artifact-free data. Following the visual inspection, the Neuroguide software options to automatically identify and reject EEG patterns consistent with artifacts relating to drowsiness and eye muscle movements were employed. By following this procedure, the Neuroguide software uses the artifact-free data from the manually identified ten second sample as a reference. With this artifact-free reference in place, the automated software program identifies and selects artifact-free data from the whole three-minute data file and discards all portions of the data with artifacts; thus, yielding artifact free samples for each participant.

Coherence measures between electrodes were obtained through qEEG Neuroguide automated processes. The Neuroguide software contains a database with information from 625 individuals, covering the age range two months to 82.6 years (Johnstone & Gunkelman, 2003), pp. 42-43). By sourcing this database, Neuroguide yields reports which provide coherence values in raw Z-score units. Utilizing standardized coherence values, discrepancies in coherence due to age-

related/developmental differences can be minimized. A subsequent automated procedure utilizing Low Resolution Electromagnetic Tomography (LORETA) was performed in Neuroguide to convert the data into a format that produces standardized coherence values between each of the 52 Brodmann Areas (BAs) in each hemisphere.

LORETA is one of the most extensively used algorithms for localizing the source of EEG signal detected on the scalp (Grech et al., 2008). By running the LORETA program on the EEG dataset from the current study, 3-dimensional statistical maps were generated to model the distribution of brain coherence values. LORETA attributes electrode activity to specific BAs by plotting the points on a standardized MRI atlas, it has demonstrated its ability to provide accurate estimations of activity in subcortical structures with better temporal resolution than can be provided by PET or fMRI (Pascual-Marqui, Michel, & Lehmann, 1994). The current study utilized the LORETA program to convert the obtained values of coherence between scalp electrodes into coherence values between each of the 52 BAs in each hemisphere. Arsalidou & Taylor (2011) proposed a neurological model based on fMRI research findings that suggest BA 40 is crucially implicated in mathematics cognitive processing. By obtaining models of EEG activity based on an MRI atlas, the current study utilized the findings by Arsalidou & Taylor (2011) to provide a framework for which the subsequent analyses would be based off of.

MATLAB 2018a (*Mathworks, Inc.*, 2018) was utilized to extract the coherence data between BA 40 and all other BAs from the full dataset. This data was then exported to Microsoft Excel and IBM SPSS (version 24; *IBM SPSS Statistics for Windows*, 2017) for final analyses. Using IBM SPSS (*IBM SPSS Statistics for Windows*, 2017), coherence values were collapsed across all participants for each BA. Principle component analyses

(PCA) with varimax rotation was applied individually to coherence values across each frequency band of interest (delta, theta, alpha 1, alpha 2, beta 1, beta 2, beta 3, and high-beta) for BA 40 in the left hemisphere then again separately in each frequency for BA 40 in the right hemisphere. PCA was applied in order to reduce the number of EEG coherence variables, thus facilitating a more accurate interpretation of the coherence properties between whole brain regions in either hemisphere rather than the individual BAs.

PCA is a traditional method that is used in EEG analysis due to the high number of variables EEG produces. PCA has been used in previous research in order to achieve similar analytic goals to the ones in the current study (Vigário, Sarela, Jousmiki, Hamalainen, & Oja, 2000). For the current study, only components whose Kaiser-Meyer-Olkin (KMO) measure of sampling adequacy was at or above the recommended value (KMO = .60) (Dziuban & Shirkey, 1974), had eigenvalues greater than 1.0 (Gorsuch, 1983; Stevens, 1996), and that passed the scree test (Bro & Smilde, 2014) were considered in the ensuing analyses.

PCA revealed that BA 40 -- implicated in quantity representation (Arsalidou & Taylor, 2011) -- was involved in components across various frequencies in both hemispheres. Subsequent bivariate Pearson's correlation coefficients were computed to quantify the correlation between these EEG coherence parameters and math ability. The components whose correlations were significant with at least two of the three WJ-III Ach math subtests ($p < .05$) were considered in subsequent regression analyses to assess their utility in predicting math scores.

After determining components that were significantly correlated with at least two of the three math subtests on the WJ-III Ach, a figure to visually depict the BAs comprising each component was generated (Figure 3.1). Figure 3.1 was created through a multi-step process beginning with the Brodmann's Interactive Atlas 1.1 brain drawing (Bernal & Perdomo, 2008). This anatomical brain atlas is derived from the brain template and Brodmann's segmentation included in the MRIcro software package (Rorden, 2005). To create Figure 3.1, the Brodmann's Atlas brain drawing was manually edited with Adobe Photoshop to display an overlay that highlights (in blue) the Brodmann areas that are included within each coherence component.

Table 2.1. Sample Descriptive Statistics for WJ-III Ach Standard Scores

	Standard Scores		
	Mean	SD	Min/Max
Calculation	101.35	20.3	52/148
Math Fluency	103.33	17.6	60/145
Applied Problems	93.5	16.3	67/134
Letter Word ID	104.1	15.49	56/135
Reading Fluency	105.63	18.63	59/148
Understanding Directions	99.92	12.34	67/124
Story Recall	107.17	15.12	71/139
Spelling	100.32	21.56	49/148
Passage Comprehension	99.47	15.12	53/133

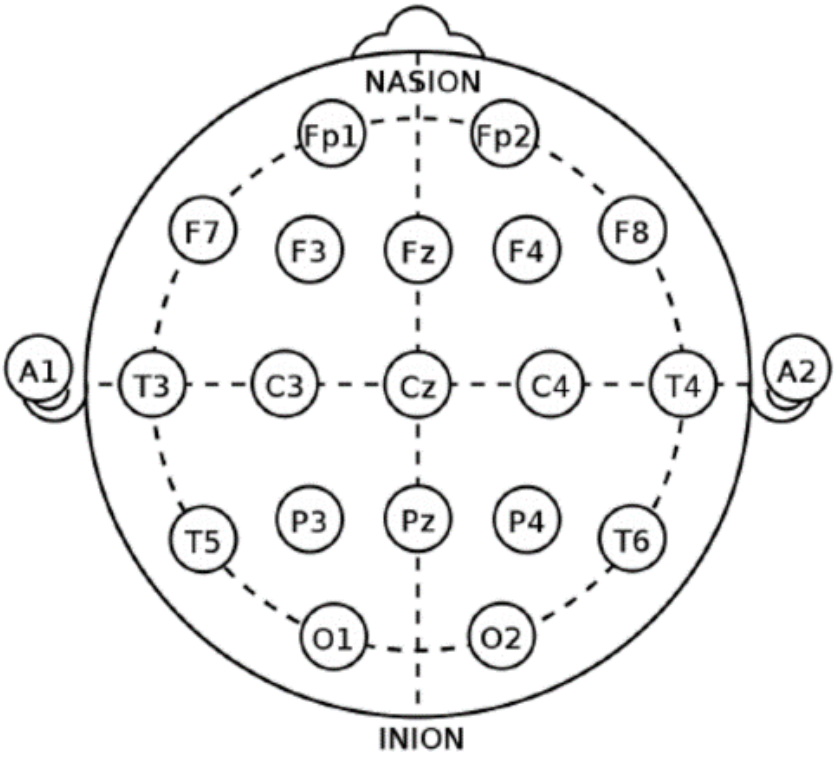

Figure 2.1: The international 10-20 system for electrode placement on the scalp defines a set of standard positions that results can be related to. In this image up is towards the front of the head.

CHAPTER 3

RESULTS

Descriptive statistics for participants' standard scores on the WJ-III Ach are reported in Table 2.1. This table includes the means, standard deviations, minimum and maximum scores. Examination of the descriptive statistics indicates that the current study has successfully included a sample of participants whose achievement scores are generally representative of the distribution of scores observed in the population.

Principle Component Analysis

Components with eigenvalues greater than 1.0, that passed the scree test, and had a KMO value greater that .60 were extracted separately for each frequency band in both brain hemispheres using varimax rotation. In the right hemisphere, several components that included BA 40 were identified in each frequency band. Within the alpha 1 band, the first three components were extracted based on the criteria above. Initial eigenvalues for these three components indicated that they explained 64%, 10%, and 8% of the variance, respectively. Within the alpha 2 band, the first three components were extracted. Initial eigenvalues for these three components indicated that they explained 59%, 13%, and 9% of the variance, respectively. The beta 1 band also had three components extracted. The eigenvalues for these components signified that they explained 24%, 16%, and 13% of the variance respectively. The beta 2 band had an additional three components extracted based on the criteria outlined above. These components' initial eigenvalues explained 36%, 14%, and 10% of the variance, respectively. Within beta 3 band, three components

were extracted; their initial eigenvalues explained 37%, 16%, and 14% of the variance respectively. In the high-beta frequency band, three components were extracted. The initial eigenvalues for these three components explained 42%, 15%, and 12% of the variance, respectively. Within the delta band, two components were extracted. They explained 37% and 14% of the variance, respectively. Theta was the final frequency band examined in the right hemisphere, within this band four components were extracted. Their initial Eigenvalues explained 34%, 13%, 11%, and 9% of the variance respectively.

The left hemisphere analyses also identified several components that included BA 40 in each frequency band. Within the alpha 1 band, the first three components were extracted based on the criteria outlined above. Eigenvalues for these three components indicated that they explained 59%, 13%, and 9% of the variance, respectively. Within the alpha 2 band, the first two components were extracted. Eigenvalues for these two components indicated that they explained 54% and 18% of the variance, respectively. The beta 1 band had three components extracted. The eigenvalues for these components signified that they explained 29%, 15%, and 12% of the variance, respectively. The beta 2 band had a total of three components extracted. These components explained 28%, 17%, and 14% of the variance, respectively. Within the beta 3 band, three components were extracted; they explained 43%, 13%, and 10% of the variance, respectively. In the high-beta frequency band, two components were extracted. These two components explained 44% and 13% of the variance, respectively. Within the delta band, two components were also extracted. They explained 47% and 14% of the variance, respectively. Lastly, the theta frequency band yielded and additional three components. These components explained 31%, 16%, and 14% of the variance, respectively.

Pearson's Correlations

Pearson's correlations were used to examine the linear relationships between the 45 extracted EEG components (listed previously) and the WJ-III Ach math scores. Table 3.2 shows the results of this analysis. There were a total of four coherence components that were significantly correlated with at least two of the three math achievement standard scores; 10 of the correlations were positive while one of them was negative, equating to a total of 11 significant correlations between the four extracted components and the three math achievement standard scores. The aim for this analysis was to identify components with correlations to multiple math achievement variables for subsequent regression analyses.

In the right hemisphere there were significant correlations ($p<.05$) between two components (one component in alpha 1 and one component in theta) and all three math achievement standard scores. Component number one in the alpha 1 band had positive correlations with all three math subtests (Calculation $r(58)=0.330$, $p < .05$, Math Fluency $r(58)=0.314$, $p < .05$, and Applied Problems $r(58)=0.290$, $p < .05$). Component number four in the theta band had significant negative correlations with all the three math subtests (Calculation $r(58)= -0.343$, $p < .01$ and Math Fluency $r(58)= -0.414$, $p < .01$, and Applied Problems $r(58)= -0.434$, $p < .01$)

In the left hemisphere, there were significant correlations ($p<.05$) among an additional two components (one component in delta and one component in theta) and at least two of the three math achievement standard scores. Component number one in the delta band had significant correlations with all three subtests (Calculation ($r(58)=.345$, $p < .01$), Math Fluency ($r(58)=.360$, $p < .01$, Applied Problems ($r(58)=.365$, $p < .01$).

Component number one in the theta band also had significant correlations with the Calculation and Math Fluency subtests, but not Applied Problems (Calculation $r(58) = 0.289$, $p < .05$ and Math Fluency $r(58)=0.351$, $p < .01$). Tables 3.3 - 3.6 show the percentage of variance explained for the initial eigenvalues in each frequency band that contains one of these significantly correlated components; tables 3.7 - 3.10 provide a summary of the rotated component loading weights of each variable in these components that are significantly correlated math standard scores.

Simple Linear Regression

Simple linear regression models were used to examine the predictive utility of each component for each of the 11 correlations (mentioned previously). Results of the significant regression models can be seen in Table 3.11.

For the Calculation subtest, all four of the identified coherence components had the ability to significantly predict performance. Likewise, all four of the components showed significant predictive utility for performance on the Math Fluency subtest. For the Applied Problems subtest, three of the four components had significant predictive utility, where the theta component in the left hemisphere did not meet statistical significance for predicting this standard score.

When examining the BAs associated with each of these predictive coherence components, several brain regions were observed to have statistical importance. The brain regions that are coherent with BA 40 include the left frontotemporal cortex (delta frequency), the left occipitotemporal cortex (theta frequency), the whole right hemisphere (alpha 1 frequency), and the right medial prefrontal cortex (theta frequency), thus coherence between these regions and BA 40 in their respective frequency bands is

assumed to have predictive utility for math performance in children. Figure 3.1 provides a graphic depicting the BAs that comprise each of the four components.

Multiple Regression

In order to determine if a greater amount of the variance in predicting specific math standard scores with these components could be explained, multiple regression models were to include each of the significant components for each model. For the Calculation subtest a multiple linear regression was calculated to predict Calculation standard scores based on the coherence value for the right alpha 1 component, the coherence value for the right theta component, the coherence value for the left delta component, and the coherence value for the left theta component. A significant regression equation was found for Calculation standard scores explaining 24% of the variance ($F(4,55) = 4.352$, $p < .01$), with an R^2 of 0.24. Participants' predicted Calculation standard score is equal to 101.350 + 4.754 - 3.067+ 1.923 + 4.936, where each component is measured in standardized coherence values. In this model, only the right alpha 1 component was indicated to be a significant predictor ($p < 0.05$) of Calculation standard score, though the variance inflation factors (VIFs) for all variables were less than two.

For the Math Fluency subtest an additional multiple linear regression model was calculated to predict the Math Fluency standard scores based on the coherence value for the right alpha 1 component, the coherence value for the right theta component, the coherence value for the left delta component, and the coherence value for the left theta component. A significant regression equation was found explaining 28% of the variance ($F(4,55) = 5.442$, $p < .01$), with an R^2 of 0.28. Participants' predicted Math Fluency standard score is equal to 93.5 + 2.851 - 3.738 + 3.519 + 2.585, where each component is

measured in standardized coherence values. In this model, none of the components were indicated to be significant predictors ($p < 0.05$) of Math Fluency standard scores, though the (VIFs) for all variables were less than two.

Lastly, a multiple linear regression model was calculated to predict Applied Problems standard scores based on the coherence value for the right alpha 1 component, the coherence value for the right theta component, and the coherence value for the left delta component. A significant regression equation was found explaining 27% of the variance ($F(3,56) = 6.786$, $p < .01$), with an R^2 of 0.27. Participants' predicted Math Fluency standard score is equal to 103.333 + 3.24 - 5.074 + 4.264, where each component is measured in standardized coherence values. In this model, only the right theta component was indicated to be a significant predictor ($p < 0.05$) of Applied Problems standard scores, though the (VIFs) for all variables were less than two.

Table 3.1. Correlations between math achievement variables and coherence components

Meausures	Alpha 1 Component 1, Right Hemisphere	Theta Component 4, Right Hemisphere	Delta Component 1, Left Hemisphere	Theta Component 1, Left Hemisphere
1. Calculation	0.33*	-0.34*	0.35*	0.29*
2. Math Fluency	0.31*	-0.41*	0.36*	0.35*
3. Applied Problems	0.29*	-0.43*	0.37*	0.22

***** Correlation is significant at the 0.05 level (2-tailed).

Table 3.2. Total variance explained by right alpha 1 band components

	Initial Eigenvalues		
Component	Total	% of Variance	Cumulative %
*1	26.763	63.721	63.721
2	4.393	10.460	74.182
3	3.310	7.880	82.061

* component significantly correlated with math subtest scores

Table 3.3 Total variance explained by right theta band components

	Initial Eigenvalues		
Component	Total	% of Variance	Cumulative %
*1	14.119	33.616	33.616
2	5.613	13.656	46.981
3	4.621	11.002	57.983
4	3.615	8.607	66.590

* component significantly correlated with math subtest scores

Table 3.4 Total variance explained by left delta band components

	Initial Eigenvalues		
Component	Total	% of Variance	Cumulative %
*1	19.359	47.218	47.218
2	5.872	14.322	61.539

* component significantly correlated with math subtest scores

Table 3.5 Total variance explained by left theta band components

	Initial Eigenvalues		
Component	Total	% of Variance	Cumulative %
*1	12.547	30.603	30.603
2	6.413	15.642	46.245
3	5.650	13.779	60.025

* component significantly correlated with math subtest scores

Table 3.6 Rotated component matrix for alpha 1 component # 1 in the right hemisphere

Variables	**Loading Weights**
Broadmann Area 40 to Amy	0.950
Broadmann Area 40 to Hip	0.947
Broadmann Area 36 to 40	0.946
Broadmann Area 28 to 40	0.945
Broadmann Area 34 to 40	0.941
Broadmann Area 38 to 40	0.924
Broadmann Area 35 to 40	0.916
Broadmann Area 30 to 40	0.907
Broadmann Area 27 to 40	0.894
Broadmann Area 20 to 40	0.874
Broadmann Area 31 to 40	0.865
Broadmann Area 21 to 40	0.828
Broadmann Area 18 to 40	0.825
Broadmann Area 23 to 40	0.824
Broadmann Area 17 to 40	0.808
Broadmann Area 7 to 40	0.807
Broadmann Area 19 to 40	0.806
Broadmann Area 37 to 40	0.805
Broadmann Area 40 to 47	0.745
Broadmann Area 24 to 40	0.654
Broadmann Area 40 to 45	0.639
Broadmann Area 13 to 40	0.615
Broadmann Area 25 to 40	0.589
Broadmann Area 5 to 40	0.579
Broadmann Area 6 to 40	0.571
Broadmann Area 10 to 40	0.539
Broadmann Area 33 to 40	0.533
Broadmann Area 40 to 44	0.529
Broadmann Area 11 to 40	0.464
Broadmann Area 32 to 40	0.460
Broadmann Area 9 to 40	0.455
Broadmann Area 40 to 46	0.428
Broadmann Area 8 to 40	0.426
Broadmann Area 22 to 40	0.346

Table 3.7 Rotated component matrix for theta component # 4 in the right hemisphere

Variables	**Loading Weights**
Broadmann Area 11 to 40	0.937
Broadmann Area 25 to 40	0.915
Broadmann Area 24 to 40	0.905
Broadmann Area 32 to 40	0.796
Broadmann Area 6 to 40	0.483
Broadmann Area 10 to 40	0.456
Broadmann Area 37 to 40	0.303

Table 3.8 Rotated component matrix for delta component #1 in the left hemisphere

Variables	Loading Weights
Broadmann Area 40 to 45	0.908
Broadmann Area 40 to 44	0.879
Broadmann Area 40 to 47	0.850
Broadmann Area 38 to 40	0.835
Broadmann Area 34 to 40	0.820
Broadmann Area 40 to Amy	0.780
Broadmann Area 28 to 40	0.763
Broadmann Area 40 to Hip	0.735
Broadmann Area 21 to 40	0.712
Broadmann Area 20 to 40	0.606
Broadmann Area 18 to 40	0.553
Broadmann Area 19 to 40	0.547
Broadmann Area 24 to 40	0.520
Broadmann Area 25 to 40	0.502
Broadmann Area 40 to 46	0.473
Broadmann Area 32 to 40	0.462
Broadmann Area 35 to 40	0.456
Broadmann Area 33 to 40	0.417
Broadmann Area 27 to 40	0.412
Broadmann Area 11 to 40	0.354
Broadmann Area 10 to 40	0.340
Broadmann Area 30 to 40	0.326
Broadmann Area 3 to 40	0.317
Broadmann Area 1 to 40	0.316
Broadmann Area 13 to 40	0.309

Table 3.9 Rotated component matrix for theta component # 1 in the left hemisphere

Variables	**Loading Weights**
Broadmann Area 40 to Hip	0.923
Broadmann Area 20 to 40	0.907
Broadmann Area 28 to 40	0.884
Broadmann Area 21 to 40	0.877
Broadmann Area 40 to Amy	0.863
Broadmann Area 19 to 40	0.802
Broadmann Area 34 to 40	0.762
Broadmann Area 18 to 40	0.757
Broadmann Area 27 to 40	0.741
Broadmann Area 30 to 40	0.715
Broadmann Area 35 to 40	0.710
Broadmann Area 38 to 40	0.656
Broadmann Area 31 to 40	0.474
Broadmann Area 40 to 47	0.466
Broadmann Area 40 to 45	0.443
Broadmann Area 23 to 40	0.304

Table 3.10 Significantly predictive coherence components for WJ-III Ach math standard scores

Calculation Subtest				
Variable		**β**	**t**	**p**
(constant)	101.35			
R Alpha 1 Comp.		0.33	7.1	0.01
Variable		**β**	**t**	**p**
(constant)	101.35			
R Theta Comp.		-0.343	7.74	0.01
Variable		**β**	**t**	**p**
(constant)	101.35			
L Delta Comp.		0.345	7.78	0.01
Variable		**β**	**t**	**p**
(constant)	101.35			
L Theta Comp.		0.289	5.3	0.03

Math Fluency Subtest				
Variable		**β**	**t**	**p**
(constant)	93.5			
R Alpha 1 Comp.		0.314	6.336	0.015
Variable		**β**	**t**	**p**
(constant)	93.5			
R Theta Comp.		-0.414	12	0.001
Variable		**β**	**t**	**p**
(constant)	93.5			
L Delta Comp.		0.36	8.656	0.005
Variable		**β**	**t**	**p**
(constant)	93.5			
L Theta Comp.		0.351	8.17	0.006

Applied Problems Subtest				
Variable		**β**	**t**	**p**
(constant)	103.33			
R Alpha 1 Comp.		0.29	5.31	0.025
Variable		**β**	**t**	**p**
(constant)	103.33			
R Theta Comp.		-0.434	13.47	0.001
Variable		**β**	**t**	**p**
(constant)	103.33			
L Delta Comp.		0.365	8.892	0.004

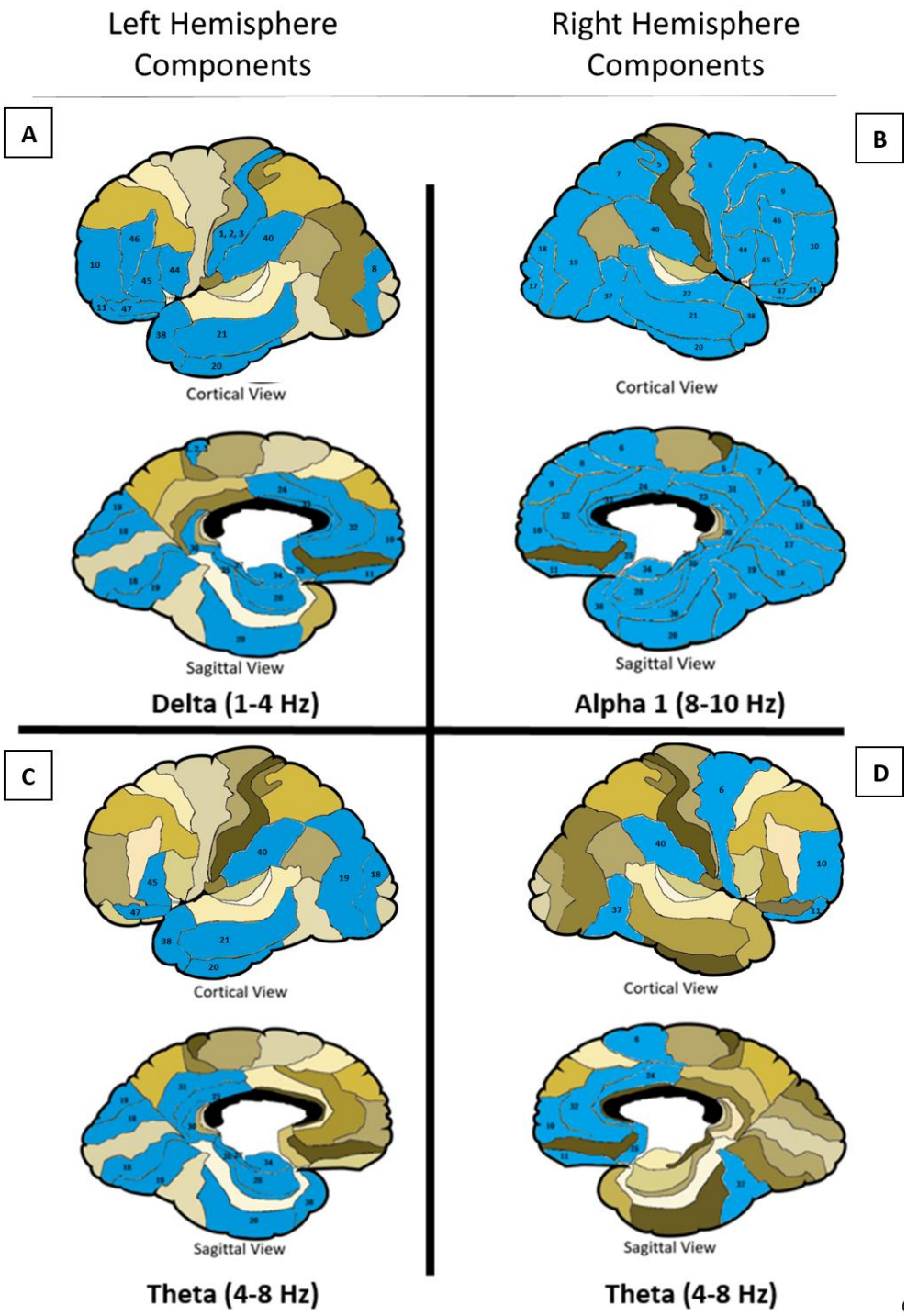

Figure 3.1: Predictive coherence components **A**: delta component 1, left hemisphere; **B**: Alpha 1 component 1, right hemisphere; **C:** theta component 1, left

CHAPTER 4

DISCUSSION

The present study investigated qEEG coherence patterns in school-aged children with and without math learning problems. This research is important because of a void in the research literature examining the neurocognitive underpinnings of the brain functions that are implicated in mathematical abilities in children. QEEG measures, such as coherence, can provide a bio-signature to: 1) clarify a true math LD (versus a more global cognitive deficit), 2) better distinguish between subtypes of math LD, and 3) direct and guide the intervention process for students with an LD. Because mathematics skills are imperative for a person's future academic and vocational success (Garnett, 1998; Ritchie & Bates, 2013), improving our ability to quickly and accurately determine a child's aptitude for mathematics is particularly salient.

Research has long supported the notion that BA 40, also known as the IPL, plays a major role in the cognitive processes surrounding math performance (Anderson et al., 2011; Cohen et al., 2000; Kroger et al., 2008). Equipped with this foundational research, the current study sought to determine how intrahemispheric brain connectivity levels at rest between BA 40 and its respective hemisphere impact a child's mathematics performance. The current study modeled the distribution of brain coherence throughout the entire brain and PCA was used to extract BA 40 coherence networks in each frequency band. These networks were then put into regression models to determine their prognostic utility for reliably predicting standardized math achievement scores.

Results indicated that there were two significant coherence networks in each hemisphere that were correlated with math ability as determined by the WJ-III Ach test battery. In the right hemisphere a coherence network in the alpha 1 frequency band (8-10 Hz) significantly predicted standard scores across the Calculation, Applied Problems, and Math Fluency subtests. This network is comprised of much of the entire right hemisphere (Table 3.4.1; Figure 3.1 B). Similarly, in the right hemisphere, an additional coherence network in the theta frequency band (4-8 Hz) was predictive of these three math standard scores. This network included BA 40 and various BAs situated in the medial prefrontal cortex (Table 3.4.2; Figure 3.1 D). In the left hemisphere, a coherence network in the delta frequency band (1-4 Hz) was predictive of all three math subtests; it included BA 40 and various BAs in the frontotemporal cortex (Table 3.4.3; Figure 3.1 A), while an additional component was predictive of the Calculation and Math Fluency subtests, but not the Applied Problems subtest. This component was in the Theta frequency band (4-8 Hz) and included BA 40 and various BAs in the occipitotemporal cortex (Table 3.4.4; Figure 3.1 C).

Interestingly, the occipitotemporal cortex is one of the main anatomical areas hypothesized to have a functional specialization for visual number processing based on fMRI research (Schmithorst & Brown, 2004). This is crucially important for the implications of the current study's findings because having increased coherence among this region at rest can imply that a child will more easily utilize this network when an environmental task demands him/her to do so. Thus, more coherence within this "math brain region" while not performing a math task is likely indicative of a more developed and "well-tuned" neurocognitive math system.

Based off of the regression models for the right hemisphere, one could surmise that having more alpha 1 coherence across the entire hemisphere and less theta coherence between BA 40 and the medial prefrontal region are beneficial for a child aiming to excel in mathematics. Likewise, in the left hemisphere, having more Delta coherence between BA 40 and the frontotemporal cortex as well as more theta coherence between BA 40 and the occipitotemporal cortex are beneficial for improved math skills in children. These results provide a framework upon which researchers can build their theoretical understanding of how child brains do math and the neurocognitive processes that underlie the math skills involved.

To further investigate specific math skillsets (e.g. calculation skills, math fluency skills, and applied problem skills, as assessed by the WJ-III Ach) and the brain activity associated with them, models including coherence networks and their respective correlated math subtest standard scores were examined through multiple linear regression analyses. Results revealed three statistically significant regression models, one for each of the math subtests. The Calculation standard scores were significantly predicted by a brain coherence model displaying greater alpha 1 coherence across the right hemisphere and less theta coherence with right medial prefrontal cortex in the presence of more delta and theta coherence between left BA 40 and the left frontotemporal and occipitotemporal cortices respectively. Similar regression models were used for the Math Fluency and Applied Problems standard scores, though the model for Applied Problems did not include the left theta component as it was not determined to be significantly correlated to this subtest.

Though all three models were examined with the same coherence networks (except for the Applied Problems model, which excluded the left theta component), neurological information specific to the math skills required by these different subtests may still be gleaned by examining the standardized beta weights for the coherence networks in each of these models. In the Calculation subtest model, increased theta coherence between left BA 40 and the left superior temporal lobe had the most influence on the model predicting Calculation standard scores. While the Math Fluency subtest model revealed that having less theta coherence between right BA 40 and the frontoparietal lobe was most influential in predicting Math Fluency standard scores. Similarly, the Applied Problems subtest model indicates that having less theta coherence between right BA 40 and the frontoparietal lobe was most influential in predicting these standard scores.

By evaluating these models and examining the influence that each of these individual coherence networks has on the model's overall prognostic utility, one's theoretical understanding in how a child's brain does math tasks specific to each of the subtests, and the neurocognitive processes that underly them, is augmented. For example, one may surmise that increased theta coherence at rest between right BA 40 and the right medial temporal cortex negatively impacts the neurocognitive processes required to perform math, but less so when performing general calculation tasks than when performing a math fluency and/or applied problems task. Essentially, these models suggest that different demands on brain connectivity may be placed on a child's brain depending on the type of math skills needing to be performed. Likely, a child's default brain connectivity, and their brain's ability to utilize appropriate networks that have

already been established, will influence their ability to perform specific math tasks with precision.

Limitations

Despite including a sample of children representing a large range of math achievement abilities, the current study accomplished this by combining two equally sized groups (half determined to have a MLD, half determined to be typically developing). By collapsing across the two groups, the study sample became unrepresentative of the population of actual students, as half the population does not score below the 25th percentile on the WJ-III Ach Math Calculation test and/or Math Fluency test.

An additional limitation exists because coherence differences between participants who achieved low math scores were not compared to high achieving participants. While these subsets of the sample were operationally defined based on the inclusion criteria of the study, findings would be difficult to generalize to MLD students since there are a variety of techniques employed across schools to define a child as MLD (Van Luit & Toll, 2018). Still, examining differences among high performers and low performers could yield valuable results, but was not pursued in the current study do to the relatively large number of EEG variables obtained and the small sample of participants that would exist in each sample had the current sample been divided into two subsets.

Moreover, due to the inclusion of such a large number of variables involved in the PCA, the current study only examined intrahemispheric coherence and did not inspect interhemispheric coherence; doing so would add an exponentially greater number of coherence variables. This is a major limitation of the current study considering there is

research to suggest that individuals who are gifted in math exhibit heightened interhemispheric connectivity compared to individuals who do not have exceptional math skills (O'Boyle, 2005). Thus, there are likely additional PCA components that would increase the prognostic utility of the methods outlined in the current study.

Another major limitation of the current study involves the interpretation of the results. How the results are currently understood relies upon the interpretation that a coherence network correlating with a math score is indicative of a network that is directly involved in the performance of that math task. In actuality, the four identified networks represent resting-state electrophysiological activity and resting-state activity does not imply that these networks are involved with the math tasks they are correlated with, nor that they become active during the performance of that math task. Despite this limitation, the point remains that these networks are, in fact, predictive of math performance, though the interpretation of their function cannot be surmised and therefore warrants continued research.

Future directions

Future neuroimaging research should aim to identify the function of the four coherence networks outlined in the current study. This can be achieved through functional neuroimaging techniques such as ERP, fNIRS, fMRI, etc. Since prior research has suggested that mathematics skills rely on several vital cognitive factors, such as planning skills, attention, processing speed, working memory, and number sense (Van Luit & Toll, 2018), future studies may also aim to determine which aspects of cognition, if any, each of the identified coherence networks are associated with. Similar analyses to the ones described in the current study should also be conducted to validate the current

study's findings and expand upon them by including variables representing interhemispheric coherence. Future research should aim to identify if interhemispheric PCA components exist and, if so, determine if they can be used to predict math performance. Moreover, BAs in addition to BA40 may also warrant further investigation to explore their role in predicting a child's math ability. To expand the clinical utility of the current study's findings, future studies should pursue neurofeedback interventions aimed to reinforce the coherence patterns that are consistent with enhanced math performance, which are outlined in the current study.

Conclusion

The current study identified four intrahemispheric components that significantly predict children's mathematics achievement. Utilizing the methods of EEG implementation and analysis outlined in the current study can lead to enhanced practices in identifying of children with math disabilities. By determining which brain regions are in sync with one another at rest we can extract networks based on the brain regions that are in coherence with one another. Further, we may determine if the coherence within a particular network has prognostic utility for predicting performance on math related tasks. Because qEEG obtains measures directly from the brain, the interpretation of EEG results can be largely objective. Utilizing an objective measure, such as qEEG coherence, in conjunction with current neuropsychological and psychoeducational testing practices, helps to mitigate the potential for human error that is inherent in diagnosing an LD. In the school context, if implemented properly, this can lead to a reduction in the incidence of false positives and negatives in LD identification, a major goal for school districts across the nation. In addition to reducing identification errors, utilizing qEEG as method of

screening for individuals who may be at risk for a MLD produces the potential for a more timely LD identification process. This would allow clinicians the opportunity to intervene much sooner, thus leading to improved overall outcomes for afflicted students (Garnett, 1998; Ritchie & Bates, 2013). Due to the exploratory nature of the current study, findings warrant continued research, yet provide a foundation for understanding some of the neurological underpinnings of math performance in children.

REFERENCES

Andersen, R. A. (1987). Inferior parietal lobule function in spatial perception and visuomotor integration. *Handbook of Physiology*, *5*(part 2).

Anderson, J. R., Betts, S., Ferris, J. L., & Fincham, J. M. (2011). Cognitive and metacognitive activity in mathematical problem solving: Prefrontal and parietal patterns. *Cognitive, Affective, & Behavioral Neuroscience*, *11*(1), 52–67.

Arns, M., Peters, S., Breteler, R., & Verhoeven, L. (2007). Different brain activation patterns in dyslexic children: Evidence from EEG power and coherence patterns for the double-deficit theory of dyslexia. *Journal of Integrative Neuroscience*, *6*(01), 175–190.

Arsalidou, M., & Taylor, M. J. (2011). Is 2+ 2= 4? Meta-analyses of brain areas needed for numbers and calculations. *Neuroimage*, *54*(3), 2382–2393.

Balu, R., Zhu, P., Doolittle, F., Schiller, E., Jenkins, J., & Gersten, R. (2015). Evaluation of Response to Intervention Practices for Elementary School Reading. NCEE 2016-4000. *National Center for Education Evaluation and Regional Assistance*.

Barry, R. J., Clarke, A. R., Johnstone, S. J., McCarthy, R., & Selikowitz, M. (2009). Electroencephalogram θ/β Ratio and Arousal in Attention-Deficit/Hyperactivity Disorder: Evidence of Independent Processes. *Biological Psychiatry*, *66*(4), 398–401. https://doi.org/10.1016/j.biopsych.2009.04.027

Berg, D. H. (2008). Working memory and arithmetic calculation in children: The contributory roles of processing speed, short-term memory, and reading. *Journal of Experimental Child Psychology, 99*(4), 288–308.

Bernal, B., & Perdomo, J. (2008, August). Brodmann's Interactive Atlas 1.1. Retrieved October 12, 2019, from http://www.fmriconsulting.com/brodmann/index.html.

Bro, R., & Smilde, A. K. (2014). Principal component analysis. *Analytical Methods, 6*(9), 2812–2831.

Burle, B., Spieser, L., Roger, C., Casini, L., Hasbroucq, T., & Vidal, F. (2015). Spatial and temporal resolutions of EEG: Is it really black and white? A scalp current density view. *International Journal of Psychophysiology, 97*(3), 210–220.

Butterworth, B., Varma, S., & Laurillard, D. (2011). Dyscalculia: From brain to education. *Science*, *332*(6033), 1049–1053.

Chen, A. C., Feng, W., Zhao, H., Yin, Y., & Wang, P. (2008). EEG default mode network in the human brain: Spectral regional field powers. *Neuroimage, 41*(2), 561–574.

Clarke, A. R., Barry, R. J., McCarthy, R., & Selikowitz, M. (1998). EEG analysis in attention-deficit/hyperactivity disorder: A comparative study of two subtypes. *Psychiatry Research*, *81*(1), 19–29.

Clarke, A. R., Barry, R. J., McCarthy, R., & Selikowitz, M. (2001). EEG-defined subtypes of children with attention-deficit/hyperactivity disorder. *Clinical Neurophysiology*, *112*(11), 2098–2105.

Cohen, L., Dehaene, S., Chochon, F., Lehericy, S., & Naccache, L. (2000). Language and calculation within the parietal lobe: A combined cognitive, anatomical and fMRI study. *Neuropsychologia*, *38*(10), 1426–1440.

D'Amico, A., & Guarnera, M. (2005). Exploring working memory in children with low arithmetical achievement. *Learning and Individual Differences*, *15*(3), 189–202.

Dehaene, S. (1992). Varieties of numerical abilities. *Cognition*, *44*(1–2), 1–42.

Dehaene, S., & Cohen, L. (1995). Towards an anatomical and functional model of number processing. *Mathematical Cognition*, *1*(1), 83–120.

Dumermuth, G. (1973). Numerical spectral analysis of the electroencephalogram. *Handbook of Electroencephalography and Clinical Neurophysiology*, *5*(Part A), 33–60.

Dziuban, C. D., & Shirkey, E. C. (1974). When is a correlation matrix appropriate for factor analysis? Some decision rules. *Psychological Bulletin*, *81*(6), 358.

Fernández, T., Harmony, T., Rodríguez, M., Bernal, J., Silva, J., Reyes, A., & Marosi, E. (1995). EEG activation patterns during the performance of tasks involving different components of mental calculation. *Electroencephalography and Clinical Neurophysiology*, *94*(3), 175–182. https://doi.org/10.1016/0013-4694(94)00262-J

Garnett, K. (1998). Math learning disabilities. *Journal of CEC*.

Gasser, T., Jennen-Steinmetz, C., & Verleger, R. (1987). EEG coherence at rest and during a visual task in two groups of children. *Electroencephalography and Clinical Neurophysiology*, *67*(2), 151–158.

Gersten, R., & Chard, D. (1999). Number sense: Rethinking arithmetic instruction for students with mathematical disabilities. *The Journal of Special Education*, *33*(1), 18–28.

González-Garrido, A. A., Gómez-Velázquez, F. R., Salido-Ruiz, R. A., Espinoza-Valdez, A., Vélez-Pérez, H., Romo-Vazquez, R., … Berumen, G. (2018). The analysis of EEG coherence reflects middle childhood differences in mathematical achievement. *Brain and Cognition*, *124*, 57–63. https://doi.org/10.1016/j.bandc.2018.04.006

Grech, R., Cassar, T., Muscat, J., Camilleri, K. P., Fabri, S. G., Zervakis, M., … Vanrumste, B. (2008). Review on solving the inverse problem in EEG source analysis. *Journal of Neuroengineering and Rehabilitation*, *5*(1), 25.

Hiebert, J., & Lefevre, P. (1986). Conceptual and procedural knowledge in mathematics: An introductory analysis. *Conceptual and Procedural Knowledge: The Case of Mathematics*, *2*, 1–27.

IBM SPSS Statistics for Windows. (2017). Armonk, NY: IBM Corp: IBM Corp.

Jäncke, L., Kleinschmidt, A., Mirzazade, S., Shah, N. J., & Freund, H.-J. (2001). The Role of the Inferior Parietal Cortex in Linking the Tactile Perception and Manual Construction of Object Shapes. *Cerebral Cortex*, *11*(2), 114–121. https://doi.org/10.1093/cercor/11.2.114

Janzen, T., Graap, K., Stephanson, S., Marshall, W., & Fitzsimmons, G. (1995). Differences in baseline EEG measures for ADD and normally achieving preadolescent males. *Biofeedback and Self-Regulation*, *20*(1), 65–82.

John, E. R., Prichep, L., Fridman, J., & Easton, P. (1988). Neurometrics: Computer-assisted differential diagnosis of brain dysfunctions. *Science*, *239*(4836), 162–169.

Johnson, D. J., & Blalock, J. W. (1987). *Adults with learning disabilities: Clinical studies*. Grune & Stratton, Incorporated.

Johnstone, J., & Gunkelman, J. (2003). Use of databases in QEEG evaluation. *Journal of Neurotherapy*, *7*(3–4), 31–52.

Koponen, T., Georgiou, G., Salmi, P., Leskinen, M., & Aro, M. (2017). A meta-analysis of the relation between RAN and mathematics. *Journal of Educational Psychology*, *109*(7), 977.

Kroger, J. K., Nystrom, L. E., Cohen, J. D., & Johnson-Laird, P. N. (2008). Distinct neural substrates for deductive and mathematical processing. *Brain Research*, *1243*, 86–103.

Lehongre, K., Morillon, B., Giraud, A.-L., & Ramus, F. (2013). Impaired auditory sampling in dyslexia: Further evidence from combined fMRI and EEG. *Frontiers in Human Neuroscience*, *7*, 454.

Margolis, A. E., Pagliaccio, D., Thomas, L., Banker, S., & Marsh, R. (2019). Salience network connectivity and social processing in children with nonverbal learning disability or autism spectrum disorder. *Neuropsychology*, *33*(1), 135.

MATLAB (Version 2018a). (2018). Natick, Massachusetts, United States: The MathWorks, Inc.

Mattingley, J. B., Husain, M., Rorden, C., Kennard, C., & Driver, J. (1998). Motor role of human inferior parietal lobe revealed in unilateral neglect patients. *Nature*, *392*(6672), 179.

Mazzocco, M. M., Feigenson, L., & Halberda, J. (2011). Impaired acuity of the approximate number system underlies mathematical learning disability (dyscalculia). *Child Development*, *82*(4), 1224–1237.

Mussolin, C., Mejias, S., & Noël, M.-P. (2010). Symbolic and nonsymbolic number comparison in children with and without dyscalculia. *Cognition*, *115*(1), 10–25.

O'Boyle, M. W. (2005). Some Current Findings on Brain Characteristics of the Mathematically Gifted Adolescent. *International Education Journal*, *6*(2), 247–251.

Pascual-Marqui, R. D., Michel, C. M., & Lehmann, D. (1994). Low resolution electromagnetic tomography: A new method for localizing electrical activity in the brain. *International Journal of Psychophysiology*, *18*(1), 49–65.

Passolunghi, M., & Cornoldi, C. (2000). Working memory and cognitive abilities in children with specific difficulties in arithmetic word problem solving. *Advances in Learning and Behavioral Disabilities*, *14*, 155–178.

Piazza, M., Facoetti, A., Trussardi, A. N., Berteletti, I., Conte, S., Lucangeli, D., … Zorzi, M. (2010). Developmental trajectory of number acuity reveals a severe impairment in developmental dyscalculia. *Cognition*, *116*(1), 33–41.

Plerou, A., & Vlamos, P. (2016). *Evaluation of Mathematical Cognitive Functions with the Use of EEG Brain Imaging*. https://doi.org/10.4018/978-1-4666-8659-5.ch014

Rippon, G., & Brunswick, N. (2000). Trait and state EEG indices of information processing in developmental dyslexia. *International Journal of Psychophysiology*, *36*(3), 251–265.

Ritchie, S. J., & Bates, T. C. (2013). Enduring links from childhood mathematics and reading achievement to adult socioeconomic status. *Psychological Science*, *24*(7), 1301–1308.

Rivera, S. M., Reiss, A., Eckert, M. A., & Menon, V. (2005). Developmental changes in mental arithmetic: Evidence for increased functional specialization in the left inferior parietal cortex. *Cerebral Cortex*, *15*(11), 1779–1790.

Rocca, M., Valsasina, P., Absinta, M., Riccitelli, G., Rodegher, M., Misci, P., … Filippi, M. (2010). Default-mode network dysfunction and cognitive impairment in progressive MS. *Neurology*, *74*(16), 1252–1259.

Rorden, C., & Brett, M. (2005). MRIcro. *Availabile online at: http://www. sph.sc. edu/comd/rorden/mricro.html*.

Satterfield, J. H., Cantwell, D. P., Lesser, L. I., & PODOSIN, R. L. (1972). Physiological studies of the hyperkinetic child: I. *American Journal of Psychiatry*, *128*(11), 1418–1424.

Savini, G., Pardini, M., Castellazzi, G., Lascialfari, A., Chard, D., D'Angelo, E., & Gandini Wheeler-Kingshott, C. A. M. (2019). Default mode network structural integrity and cerebellar connectivity predict information processing speed deficit in multiple sclerosis. *Frontiers in Cellular Neuroscience*, *13*, 21.

Schmithorst, V. J., & Brown, R. D. (2004). Empirical validation of the triple-code model of numerical processing for complex math operations using functional MRI and

group Independent Component Analysis of the mental addition and subtraction of fractions. *Neuroimage*, *22*(3), 1414–1420.

Singh-Curry, V., & Husain, M. (2009). The functional role of the inferior parietal lobe in the dorsal and ventral stream dichotomy. *Neuropsychologia*, *47*(6), 1434–1448. https://doi.org/10.1016/j.neuropsychologia.2008.11.033

Thatcher, R. W. (2011). Neuropsychiatry and quantitative EEG in the 21st Century. *Neuropsychiatry*, *1*(5), 495–514.

Thatcher, R. W., North, D., & Biver, C. (2005a). EEG and intelligence: Relations between EEG coherence, EEG phase delay and power. *Clinical Neurophysiology*, *116*(9), 2129–2141.

Thatcher, R. W., North, D., & Biver, C. (2005b). EEG and intelligence: Relations between EEG coherence, EEG phase delay and power. *Clinical Neurophysiology*, *116*(9), 2129–2141.

Thatcher, R. W., North, D. M., Curtin, R. T., Walker, R. A., Biver, C. J., Gomez, J. F., & Salazar, A. M. (2001a). An EEG severity index of traumatic brain injury. *The Journal of Neuropsychiatry and Clinical Neurosciences*, *13*(1), 77–87.

Thatcher, R. W., North, D. M., Curtin, R. T., Walker, R. A., Biver, C. J., Gomez, J. F., & Salazar, A. M. (2001b). An EEG severity index of traumatic brain injury. *The Journal of Neuropsychiatry and Clinical Neurosciences*, *13*(1), 77–87.

Thatcher, R. W., Walker, R., Gerson, I., & Geisler, F. (1989). EEG discriminant analyses of mild head trauma. *Electroencephalography and Clinical Neurophysiology*, *73*(2), 94–106.

Toll, S. W., Van der Ven, S. H., Kroesbergen, E. H., & Van Luit, J. E. (2011). Executive functions as predictors of math learning disabilities. *Journal of Learning Disabilities*, *44*(6), 521–532.

Van Luit, J. E. H., & Toll, S. W. M. (2018). Associative cognitive factors of math problems in students diagnosed with developmental dyscalculia. *Frontiers in Psychology*, *9*.

Vickery, T. J., & Jiang, Y. V. (2008). Inferior parietal lobule supports decision making under uncertainty in humans. *Cerebral Cortex*, *19*(4), 916–925.

Vigário, R., Sarela, J., Jousmiki, V., Hamalainen, M., & Oja, E. (2000). Independent component approach to the analysis of EEG and MEG recordings. *IEEE Transactions on Biomedical Engineering*, *47*(5), 589–593.